Organic–inorganic hybrids based on four-electron reduced Keggin β-isomer phosphododecamolybdates and diazines

Pablo Vitoria,[a] María Ugalde,[a] Juan M. Gutiérrez-Zorrilla,*[a] Pascual Román,[a] Antonio Luque,[a] Leire San Felices[a] and Javier García-Tojal[b]

[a] *Departamento de Química Inorgánica, Facultad de Ciencias, Universidad del País Vasco, Apartado 644, 48080, Bilbao, Spain. E-mail: qipguloj@lg.ehu.es*
[b] *Área de Química Inorgánica, Universidad de Burgos, Plaza Misael Bañuelos, s/n, 09001, Burgos, Spain*

Received (in Montpellier, France) 24th July 2002, Accepted 2nd October 2002
First published as an Advance Article on the web 19th December 2002

Six salts of diazonium cations ($C_4H_5N_2^+$) with the four-electron reduced β-Keggin phosphododecamolybdate, $(1,2\text{-}C_4H_5N_2)_3[H_4PMo_{12}O_{40}]\cdot 9H_2O$ (**1**), $(1,3\text{-}C_4H_5N_2)_2[H_5PMo_{12}O_{40}]\cdot(1,3\text{-}C_4H_4N_2)\cdot 10H_2O$ (**2**), $(1,4\text{-}C_4H_5N_2)_3[H_4PMo_{12}O_{40}]\cdot 5H_2O$ (**3**), $(1,2\text{-}C_4H_5N_2)_3[H_4PMo_{12}O_{40}]\cdot 2H_2O$ (**4**), $(1,3\text{-}C_4H_5N_2)_3[H_4PMo_{12}O_{40}]\cdot 2H_2O$ (**5**), and $(1,4\text{-}C_4H_5N_2)_2[H_5PMo_{12}O_{40}]\cdot\frac{1}{2}(1,4\text{-}C_4H_4N_2)\cdot 5H_2O$ (**6**), have been synthesised in aqueous solution. Compounds **1**–**3** were obtained photochemically using methanol as electron donor, and compounds **4**–**6** were prepared using thiophosphate as reducing agent. These compounds contain the four-electron reduced β-Keggin polyanion with a variable degree of protonation. The crystal packing in compound **1** consists of chains formed by pairs of polyanions hydrogen bonded along the [010] direction. The diazonium cations are connected, *via* NX1–HX1···Ow hydrogen bonds, to a ten-membered ring of hydrogen bonded water molecules. The crystal packing in compound **6** is formed by antiparallel chains of polyanions connected through the hydrogen bond $OH_{poly}\cdots O_{poly}$ along the [010] direction. These polyanion chains are embedded in a 3D-channel structure formed by a helicoidal arrangement of the diazine species hydrogen bonded *via* the water molecules. The dimensions of these tunnels are approximately 14 × 13.5 Å. *Ab initio* RHF calculations have been performed on idealised α- and β-Keggin isomers in order to get information about stability and protonation sites and interactions between the organic rings and the surface of the Keggin anions.

Introduction

Polyoxometalates[1] have attracted great attention in the last two decades due to their utility in catalysis,[2] medicine and biology,[3] and materials science.[4] This wide range of applications is based on 1) the ability of polyoxometalates to act as electron and proton reservoirs, and 2) the extreme variability of their molecular properties including size, shape, charge, and acidity. There are already more commercial applications of polyoxometalates than any other class of cluster compounds.[5]

The most active area of applications is catalysis, but this activity has involved only a small number of well-known polyoxometalates. In particular, the bifunctional acidic and redox properties of heteropolyanions based upon the Keggin unit structure,[6] $[X^{n+}M_{12}O_{40}]^{(8-n)-}$, have been employed in a variety of attractive processes. These include O_2 and H_2O_2-based oxidations and processes that take place under environment friendly conditions. Being nanoscopic clusters, polyoxometalates afford properties not seen in solid state heterogeneous catalysts nor in soluble monomeric homogeneous catalysts.[7]

A substantial portion of the reported homogeneous catalytic processes are photochemical in nature, where the polyoxometalates act as electron relays in electron-transfer and/or hydrogen-transfer reactions due to their ability to accept and release a variable number of electrons without decomposition.[8] The formation of reduced polyoxometalates is concomitant with this photocatalytic behaviour.

On the other hand, the synthesis of microporous materials that are exploited as catalysts in shape-selective processes is facilitated by the use of structure-directing agents.[9] These species, which are generally organic bases, can template inorganic groups to form materials with tailorable pore shapes and sizes.[10] We have explored the general applicability of the use of planar organic bases for the synthesis of organic–inorganic hybrid materials in order to obtain a better comprehension of the interaction between organic substrates and polyoxometalate catalysts.[11] The present paper reports the syntheses, crystal structures, physical properties, and *ab initio* RHF calculations of two related series of salts based on four-electron reduced β-Keggin phosphododecamolybdates and diazines.

Results and discussion

Synthesis and spectroscopic studies

Compounds **1**–**3** were photochemically prepared in aqueous solution containing methanol as electron donor at room temperature according to the reaction:

$$Na_2MO_4\cdot 2H_2O + Na_2HPO_4 \xrightarrow[2)\ MeOH\ 3)\ h\nu]{1)\ HCl\ (pH=0)} \text{blue photolyte}$$

$$\xrightarrow{\text{diazine}} (C_4H_5N_2)_x[H_yPMo_{12}O_{40}]\cdot nH_2O$$

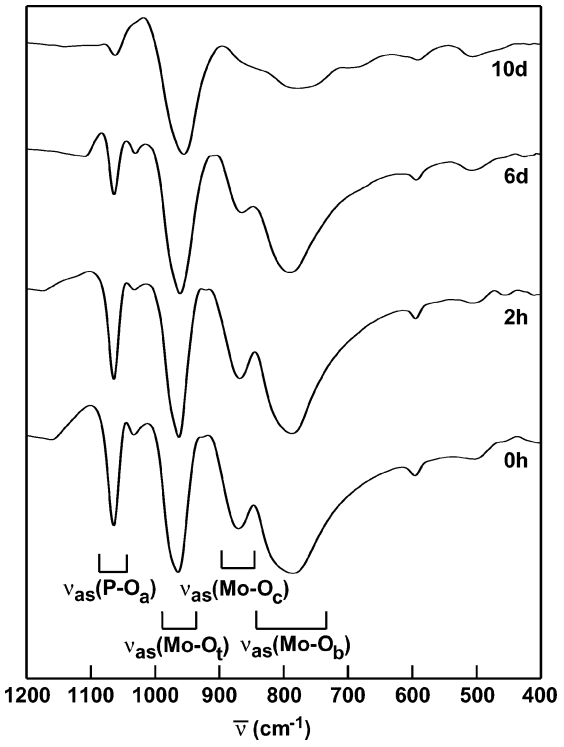

Fig. 1 Irradiation time dependence of the IR spectra of photolyte solutions.

Compounds **4**–**6** were obtained in aqueous solution using thiophosphate as reducing agent according to the reaction:

$$Na_2MO_4 \cdot 2H_2O + Na_3PO_3S \cdot 10H_2O \xrightarrow[2)\ \text{heat}]{1)\ HCl\ (pH=0)} \text{blue solution} + S_8 \xrightarrow{\text{diazine·HCl}} (C_4H_5N_2)_x[H_yPMo_{12}O_{40}] \cdot nH_2O$$

The IR spectra of the blue photolyte as a function of irradiation time are displayed in Fig. 1. The most remarkable fact is the longer the irradiation time, the stronger is the Mo–O_t stretching vibration. To try to explain these observations, *ab initio* RHF calculations have been carried out on both the oxidised and the four-electron reduced β-isomer. On reduction, the Mulliken charges increase not only on the molybdenum atoms, as expected, but also on the terminal oxygen atoms (Table 1). This means an increase in the dipole moment of the Mo–O_t bonds and, consequently, an increase in the intensity of the corresponding infrared band.[12]

Crystal structures

The most common Keggin isomer is the α-isomer. This anion consists of a central PO_4 tetrahedron surrounded by four Mo_3O_{13} groups which result from the association of three edge-sharing MoO_6 octahedra in such a way that the ideal polyanion has T_d symmetry, giving up eight trimers and six tetramers (Fig. 2).[13]

The anion in compounds **1**–**6** is the β-Keggin isomer,[14] which acquires its structure by rotating one of the edge-shared Mo_3O_{13} moieties of the α-Keggin structure by 60° around a threefold axis. This assembly is proper to the β-Keggin ion being its ideal symmetry C_{3v} (Fig. 2, bottom). The twelve MoO_6 octahedra of this isomer form eight trimers and six tetramers and can be classified structurally by three types: a) three octahedra in the 60°-rotated Mo_3O_{13} trimer, b) three octahedra in the bottom corner-shared Mo_3O_{15} triad and c) six octahedra in the Mo_6O_{27} central belt. As in the α-isomer, four types of oxygen atoms are present: O_a (the oxygen atoms linked to the phosphorus atom), O_b (the bridging oxygen atoms between two corner sharing octahedra), O_c (the bridging oxygen atoms between two edge-sharing octahedra) and O_t (the terminal oxygen atoms). Fig. 3 shows the β-Keggin anion structure together with the atom labelling.

Table 1 Mulliken charges for molybdenum and oxygen atoms in oxidised and reduced β-isomers

	Oxidised	Reduced	Δ_{red-ox}
Rotated trimer			
Mo	2.584	2.455	−0.129
O_t	−0.549	−0.715	−0.166
O_c	−0.975	−1.010 (H)	−0.035
O_b[a]	−1.081	−1.059	0.022
Central belt			
Mo	2.572	2.413	−0.159
O_t	−0.551	−0.730	−0.179
O_c	−0.937	−1.019 (H)	−0.082
O_b	−1.155	−1.107	0.048
Bottom triad			
Mo	2.583	2.437	−0.146
O_t	−0.551	−0.723	−0.172
O_c[a]	−0.980	−0.984	−0.004
O_b	−1.094	−1.097 (H)	0.003

[a] Act as connectors to the central belt. (H) Denotes protonation sites.

Selected Mo···Mo distances, Mo–O–Mo bond angles for compounds **1**, **2** and **6**, and the RHF calculations for ideal geometries are listed in Table 2. As can be seen, there are some significant dimensional differences between the α- and β-isomers. The major effect, a symmetrical shift of the molybdenum atom framework away from the anion 3-fold axis,[15] is due to the protonation of some bridging oxygen atoms which produces an enlargement of 0.14 Å in the Mo···Mo distances in the central belt, 0.20 Å in the corner-shared bottom triad and about 0.18 Å in the rotated trimer. The corner-shared Mo···Mo distances among the octahedra of the rotated trimer and the adjacent central belt are shorter than in the oxidised α-structures, but the remaining Mo···Mo separations are quite similar.

The Mo–O bond distances (Table 3) of the polyoxometalate are in the range of 1.67–1.69 Å for terminal oxygen atoms, 1.85–2.12 Å for bridging oxygen atoms and 2.40–2.54 Å for oxygens of the PO_4 group. Empirical bond length/bond number calculations, using the formula $[d(\text{Mo–O})/1.892]^{-5.74}$,[16] indicate that four oxygen atoms in compound **1** [O23, O25, and O27 (central belt), and O35 (bottom triad)], and five oxygen atoms in compounds **2** and **6** [O14 (rotated trimer), O23, O25, and O27 (central belt), and O36 (bottom triad)], are protonated. The remaining bridging oxygen atoms give a larger bond order, average 1.9(1).

Calculations on the four-electron reduced β-isomer show that the two degenerate HOMO orbitals are mainly located on the molybdenum d orbitals, but with a high participation of only the following bridging oxygen p orbitals: O13–15 (rotated trimer), O23, O25, O27 (central belt), and O34–36 (bottom triad) (Fig. 4); that is, precisely those oxygen atoms which are experimentally found to be protonated.

Protonation of oxygen atoms produces an enlargement of the Mo–O distances to about 2.10 Å. Moreover, a significant decrease in the bond angles Mo–OH–Mo is observed, from 128° to 122° in the rotated trimer, from 127° (from RHF calculation) to 116° for the edge-shared octahedra in the central belt, and from 156° to 142° in the corner-shared octahedra in the bottom triad.

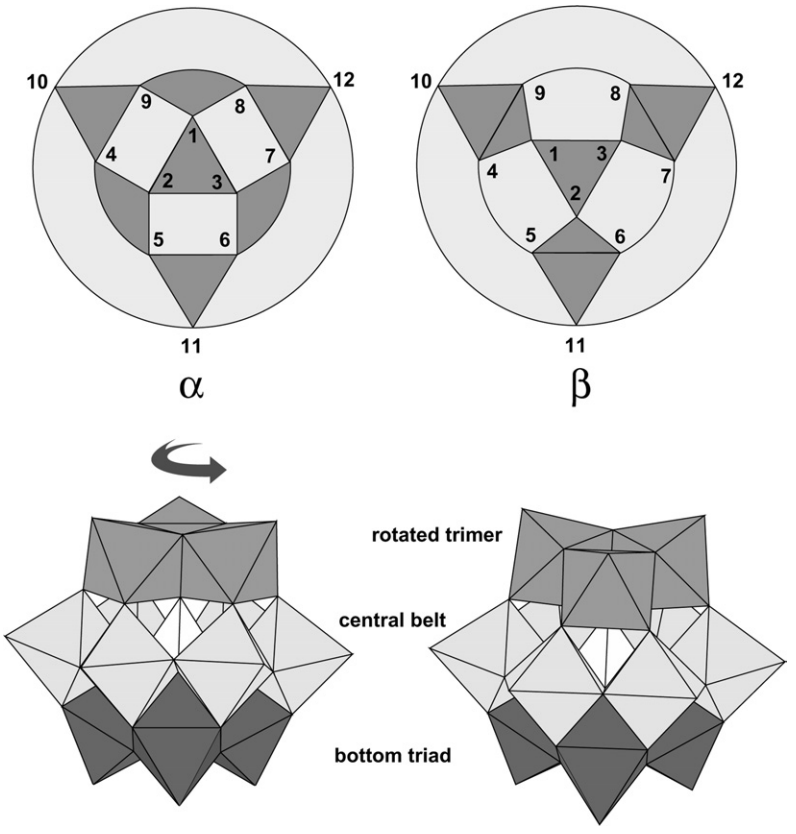

Fig. 2 (Top) Jeannin diagrams for α- and β-Keggin isomers. (Bottom) Polyhedral representations of both isomers. Trimer means three edge-shared MoO_6 octahedra and triad three corner-shared MoO_6 octahedra.

Crystal packing in compound 1. The asymmetric unit contains one β-$[H_4PMo_{12}O_{40}]^{3-}$ anion, three pyrazinium cations and nine water molecules. The crystal packing in this compound consists of chains formed by pairs of polyanions hydrogen bonded along the [010] direction. The oxygen atoms involved in the hydrogen bond network are O35 and O6, responsible for pairing the polyanions through two hydrogen bonds of the type O35–H···O6 (3.028 Å), the water molecules O41, O43, and O46, which are disposed in a chair conformation around a centre of symmetry between two pairs of β-Keggin anions, and the oxygens of polyanion O5, O7, O23, O25, and O31 (Fig. 5).

The 1,2-diazonium cations are connected, *via* NX1–HX1···Ow hydrogen bonds, to a ten-membered ring of hydrogen bonded water molecules (Fig. 6). These units are placed between the chains of polyanions acting as connectors among such chains through hydrogen bonds that involve the polyanion oxygen atoms O9, O14, O15, and O27. Moreover, the organic planar cations are disposed parallel to tetrameric units of adjacent polyanions (cations 1 and 3) and rotated trimer (cation 2). The distances from the cation's centroid to the mean plane defined by the surface oxygen atoms of the tetramer or trimer are 2.95 Å for cation 1, 2.81 Å for cation 2, and 3.16 Å for cation 3. It is remarkable that one of the cations interacts in a strong manner with the rotated trimer. This fact can be explained because, as calculated, the four-electron reduced β-isomer has a dipolar moment of 0.55 D pointing towards this rotated trimer.

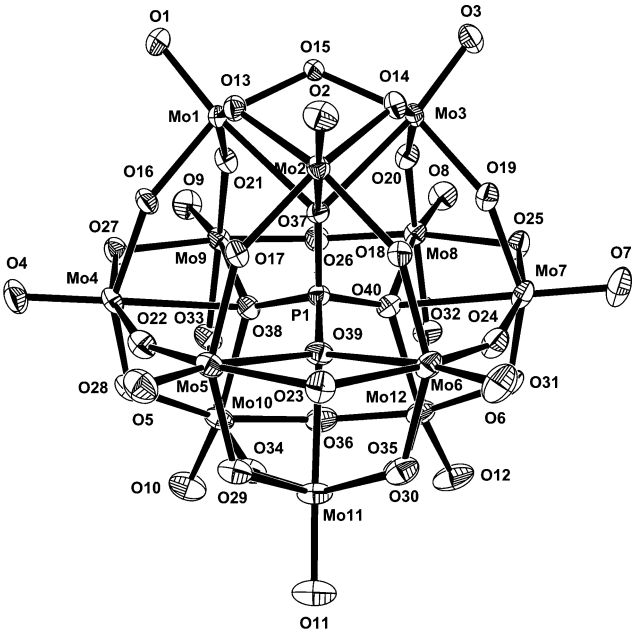

Fig. 3 ORTEP view of β-$[H_xPMo_{12}O_{40}]^{(7-x)-}$ anion with atom labelling.

Crystal packing in compound 2. The asymmetric unit consists of one β-$[H_5PMo_{12}O_{40}]^{2-}$ anion, two pyrimidinium cations, one pyrimidine molecule, and ten water molecules. The crystal packing in this compound consists of two centrosymmetrically related polyanions linked through two hydrogen bonds of type O36–H···O33 (2.875 Å). These couples are hydrogen bonded along the [010] direction through the water molecule O45, which connects the cations 2 in a helicoidal arrangement along the same direction (Fig. 7). The 1,3-diazine species are hydrogen bonded to the water molecule O44, which forms part of a "water fall" along the [010] direction with the rest of water molecules. In this compound the three organic planar rings present π interactions with the surface oxygen atoms of the tetrameric units. The distances from

Table 2 Selected Mo···Mo distances (Å) and Mo–O–Mo angles (°) for compounds **1**, **2** and **6**[a]

	β-isomer				α-isomer	
	1	**2**	**6**	RHF[b]	Diazonium salts[c]	RHF[d]
Rotated trimer[e]						
Mo1···Mo2	3.425(6)	3.435(2)	3.450(1)	3.493	3.403	3.460
Mo1···Mo3	3.423(6)	3.445(3)	3.424(1)			
Mo2···Mo3	3.433(6)	3.633(2) (H)[f]	3.600(1) (H)			
Mo1–O13–Mo2	126.5(2)	127.0(8)	128.1(2)	129.0	125.5	130.2
Mo2–O14–Mo3	127.5(3)	120.3(3) (H)	122.5(2) (H)			
Mo1–O15–Mo3	124.9(2)	129.7(8)	127.5(3)			
Central belt						
Mo4···Mo5	3.668(6)	3.686(2)	3.676(1)	3.731	3.687	3.713
Mo5···Mo6	3.557(6) (H)	3.534(3) (H)	3.549(1) (H)	3.455	3.416	3.460
Mo6···Mo7	3.663(6)	3.682(2)	3.669(1)			
Mo7···Mo8	3.572(6) (H)	3.559(2) (H)	3.577(1) (H)			
Mo8···Mo9	3.672(6)	3.684(3)	3.658(1)			
Mo4···Mo9	3.562(6) (H)	3.546(2) (H)	3.542(1) (H)			
Mo4–O22–Mo5	157.8(3)	157.8(9)	158.3(3)	164.5	151.1	154.8
Mo5–O23–Mo6	116.4(2) (H)	116.8(6) (H)	115.0(2) (H)	125.7	125.5	130.2
Mo6–O24–Mo7	156.3(3)	158.5(8)	157.9(3)			
Mo7–O25–Mo8	115.7(2) (H)	114.6(6) (H)	117.0(2) (H)			
Mo8–O26–Mo9	156.8(3)	159.6(8)	156.1(3)			
Mo4–O27–Mo9	115.5(2) (H)	117.0(6) (H)	116.6(2) (H)			
Bottom triad[e]						
Mo10···Mo11	3.717(6)	3.708(2)	3.700(1)	3.774	3.707	3.713
Mo11···Mo12	3.975(6) (H)	3.679(2)	3.689(1)			
Mo10···Mo12	3.697(6)	3.943(3) (H)	3.974(1) (H)			
Mo10–O34–Mo11	155.8(3)	156.4(9)	155.6(3)	155.3	151.4	154.8
Mo10–O36–Mo12	155.5(3)	140.9(7) (H)	141.6(2) (H)			
Mo11–O35–Mo12	142.7(3) (H)	157.5(9)	156.2(3)			

[a] Comparison with α-isomer in oxidised diazonium salts and *ab initio* RHF calculations for α and β-isomers. [b] C_{3v} symmetry. [c] Mean values in the oxidised salts of diazonium cations with a C_{3v} crystallographic symmetry. [d] T_d symmetry. [e] Trimer denotes three edge-shared MoO_6 octahedra and triad means three corner-shared MoO_6 octahedra. [f] (H) indicates protonation in one of the bridging oxygen atoms.

the cation's centroid to the mean plane defined by the eight surface oxygen atoms of the tetrameric units are 2.63 Å for cation 1 and 2.83 Å for cation 3. On the other hand, the cation 2, which forms a helicoidal chain with the water molecule O45, is sandwiched by two polyanions at distances of 2.83 and 2.80 Å, respectively.

Crystal packing in compound 6. The asymmetrical unit consists of one β-$[H_5PMo_{12}O_{40}]^{2-}$ anion, two pyrazinium cations, one pyrazine molecule, located on a centre of symmetry, and five water molecules. The crystal packing in this compound is formed by antiparallel chains of polyanions connected through the hydrogen bond O36–H···O2 (2.875 Å) along the [010] direction [Fig. 8(a)]. Polyanions belonging to adjacent chains are connected through O25–H···O4 hydrogen bonds (2.748 Å) and the water molecules O41, O42, O44, and O45 which are hydrogen bonded along the [100] direction [Fig. 8(b)]. The polyanion chains are embedded in a 3D channelled structure formed by a helicoidal arrangement of the diazine species hydrogen bonded by the water molecules O43 and O45, according to the sequence: ring 1–O45–ring 2–O43–ring 3–O43... (Fig. 9). The dimensions of these tunnels are approximately 14 × 13.5 Å.

The organic planar rings present π interactions with the surface oxygen atoms of dimeric units but not with the tetrameric units.

Weak interactions. The presence of intermolecular weak interactions between aromatic rings and tetrameric units of the Keggin anion was studied through the analysis of the charge density using the theory of atoms in molecules (AIM), which has been shown, both in experimental and theoretical studies, to be able to highlight the dominant interactions which contribute to weak binding forces.

Calculations were performed on a model of compound **2** using the crystallographically determined geometries. The system studied includes ring 1 and the tetramer comprised by the octahedra Mo6, Mo7, Mo11 and Mo12.

Besides bond critical points (CPs) in the charge density corresponding to the intramolecular bonds, several bond CPs appear connecting the ring and tetramer, and it is possible to find a critical point corresponding to a very weak hydrogen bond (Fig. 10). The value of the charge density at all these intermolecular critical points is quite small ($\sim 10^{-3}$ atomic units) and the Laplacian is small and positive, which is indicative of a closed-shell interaction and, in the particular case of this compound, of π–π interactions between the oxygen atoms of the tetramer and the aromatic cation. The properties of the charge density at the intermolecular CPs are listed in Table 4.

In order to satisfy the Poincaré–Hopf relationship: $n - b + r - c = 1$ (where n is the number of nuclei and b, r, and c are the number of bond, ring, and cage CPs, respectively), eight ring and two cage CPs appear between the tetramer and the cation. As the bond CPs display a curvature of the charge density much smaller in the direction normal to the bond path than along it, the magnitude of the electron density at the ring and bond CPs is similar, which creates a region of almost constant electron density between the anion and cation.

Table 3 Mo–O bond distances (Å) for compounds **1**, **2** and **6**[a]

	β-isomer				α-isomer	
	1	**2**	**6**	RHF[b]	Diazonium salts[c]	RHF[d]
Rotated trimer						
Mo1–O1	1.690(4)	1.67(2)	1.673(5)	1.670	1.677	1.670
Mo1–O13	1.874(4)	1.95(1)	1.976(5)	1.906	1.913	1.907
Mo1–O15	1.907(4)	1.92(2)	1.915(5)	1.906	1.913	1.907
Mo1–O16	1.935(4)	1.90(2)	1.928(5)	1.907	1.919	1.902
Mo1–O21	1.955(5)	1.90(1)	1.933(5)	1.907	1.919	1.902
Mo1–O37	2.446(5)	2.47(2)	2.457(4)	2.443	2.432	2.437
Mo2–O2	1.677(4)	1.67(1)	1.687(5)			
Mo2–O13	1.961(5)	1.89(2)	1.860(5)			
Mo2–O14	1.925(4)	2.12(1)	2.029(5)			
Mo2–O17	1.930(4)	1.87(2)	1.881(5)			
Mo2–O18	1.929(5)	1.92(2)	1.934(5)			
Mo2–O37	2.460(5)	2.44(1)	2.458(5)			
Mo3–O3	1.679(4)	1.68(2)	1.661(5)			
Mo3–O14	1.903(4)	2.07(1)	2.077(5)			
Mo3–O15	1.955(4)	1.91(2)	1.903(5)			
Mo3–O19	1.919(5)	1.93(1)	1.924(5)			
Mo3–O20	1.938(4)	1.92(1)	1.906(5)			
Mo3–O37	2.427(4)	2.48(2)	2.464(4)			
Central belt						
Mo4–O4	1.674(4)	1.65(1)	1.679(5)	1.671	1.672	
Mo4–O16	1.884(4)	1.89(2)	1.849(5)	1.895	1.924	
Mo4–O22	1.869(5)	1.88(1)	1.857(5)	1.895	1.924	
Mo4–O27	2.109(5)	2.07(1)	2.082(4)	1.910	1.914	
Mo4–O28	1.869(5)	1.95(1)	1.928(5)	1.910	1.914	
Mo4–O38	2.496(4)	2.53(1)	2.512(5)	2.426	2.430	
Mo5–O5	1.681(4)	1.66(1)	1.683(5)			
Mo5–O17	1.860(4)	1.92(2)	1.904(5)			
Mo5–O22	1.870(5)	1.87(2)	1.886(5)			
Mo5–O23	2.089(4)	2.08(1)	2.095(5)			
Mo5–O29	1.918(5)	1.88(2)	1.873(5)			
Mo5–O39	2.540(5)	2.47(1)	2.501(5)			
Mo6–O6	1.677(5)	1.68(1)	1.672(5)			
Mo6–O18	1.867(4)	1.88(2)	1.893(5)			
Mo6–O23	2.097(4)	2.07(1)	2.113(5)			
Mo6–O24	1.870(4)	1.87(1)	1.875(5)			
Mo6–O30	1.914(5)	1.87(1)	1.880(5)			
Mo6–O39	2.490(5)	2.49(1)	2.485(4)			
Mo7–O7	1.670(4)	1.69(1)	1.662(5)			
Mo7–O19	1.872(5)	1.87(2)	1.866(5)			
Mo7–O24	1.873(5)	1.88(1)	1.863(5)			
Mo7–O25	2.121(5)	2.11(1)	2.095(4)			
Mo7–O31	1.918(5)	1.88(1)	1.913(5)			
Mo7–O40	2.454(4)	2.51(1)	2.536(4)			
Mo8–O8	1.673(4)	1.65(1)	1.674(5)			
Mo8–O20	1.858(5)	1.87(1)	1.870(5)			
Mo8–O25	2.098(4)	2.12(1)	2.101(4)			
Mo8–O26	1.876(4)	1.90(1)	1.871(5)			
Mo8–O32	1.898(5)	1.89(1)	1.898(5)			
Mo8–O40	2.542(5)	2.50(1)	2.480(4)			
Mo9–O9	1.683(5)	1.68(1)	1.673(5)			
Mo9–O21	1.871(5)	1.89(2)	1.856(5)			
Mo9–O26	1.872(4)	1.84(1)	1.868(5)			
Mo9–O27	2.103(4)	2.09(1)	2.080(5)			
Mo9–O33	1.877(5)	1.92(2)	1.923(5)			
Mo9–O38	2.481(5)	2.48(1)	2.461(4)			
Bottom triad						
Mo10–O10	1.676(5)	1.69(2)	1.682(5)	1.670	1.676	
Mo10–O28	1.951(5)	1.85(1)	1.874(5)	1.908	1.909	
Mo10–O33	1.941(5)	1.95(1)	1.933(4)	1.908	1.909	
Mo10–O34	1.945(5)	1.85(1)	1.837(4)	1.910	1.917	
Mo10–O36	1.927(5)	2.11(1)	2.107(5)	1.910	1.917	
Mo10–O38	2.398(5)	2.40(1)	2.412(4)	2.451	2.425	
Mo11–O11	1.678(5)	1.68(2)	1.671(5)			
Mo11–O29	1.885(5)	1.93(1)	1.958(5)			
Mo11–O30	1.935(4)	1.95(1)	1.937(5)			
Mo11–O34	1.856(5)	1.94(2)	1.948(5)			
Mo11–O35	2.100(5)	1.92(1)	1.917(5)			
Mo11–O39	2.380(5)	2.42(1)	2.414(4)			
Mo12–O12	1.675(5)	1.65(2)	1.668(5)			
Mo12–O31	1.944(4)	1.94(1)	1.893(5)			
Mo12–O32	1.900(5)	1.94(1)	1.925(4)			
Mo12–O35	2.095(5)	1.83(1)	1.853(4)			
Mo12–O36	1.856(5)	2.07(1)	2.101(5)			
Mo12–O40	2.421(5)	2.44(1)	2.433(4)			
PO_4 unit						
P1–O37	1.532(4)	1.52(2)	1.530(5)	1.585	1.533	1.583
P1–O38	1.535(5)	1.54(1)	1.551(5)	1.588	1.530	
P1–O39	1.538(4)	1.55(1)	1.534(4)			
P1–O40	1.544(5)	1.53(1)	1.537(5)			

[a] Comparison with α-isomer in oxidised diazonium salts and *ab initio* RHF calculations for α and β-isomers. [b] C_{3v} symmetry. [c] Mean values in the oxidised salts of diazonium cations with a C_{3v} crystallographic symmetry. [d] T_d symmetry.

Conclusions

The β-isomer is the most stable form of the four-electron reduced $[H_xPMo_{12}O_{40}]^{(7-x)-}$ polyanion, as supported by experiment[14,15] and theoretical calculations.[17] This isomer shows a great tendency to protonation, due to the increased basicity of the bridging oxygen atoms. The presence of protonated oxygen atoms in the four-electron reduced polyanions allows the formation of strong hydrogen bonds between adjacent polyanions, of type O_{poly}–H···O_{poly}, which give an arrangement of polyanions in couples, as in compound **1** and **2**, or chains, as in compound **6**.

The properties of organic–inorganic compounds are strongly affected by the packing pattern of the components in the solid. Compounds containing organic planar cations and bulky Keggin anions adopt two different packing arrangements: (a) based on alternating layers of organic donors and Keggin polyoxoanions and (b) based on alternating arrangements of cations and anions.[18] While packing type (b) is present in compound **1** and **2**, like in the oxidised salts, where the diazonium cations are disposed parallel to the tetrameric or rotated trimeric units, the packing of compound **6** does not belong to any of the above mentioned models. This fact could be explained by the high rigidity imposed by the

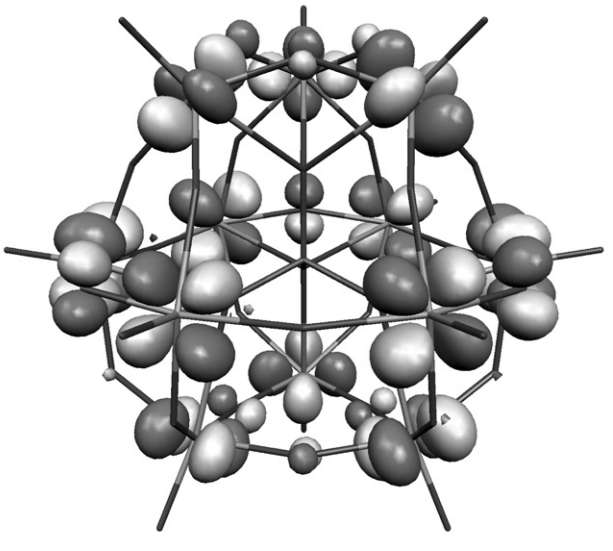

Fig. 4 Superposition of double-degenerated HOMO orbitals in the four-electron reduced Keggin β-isomer.

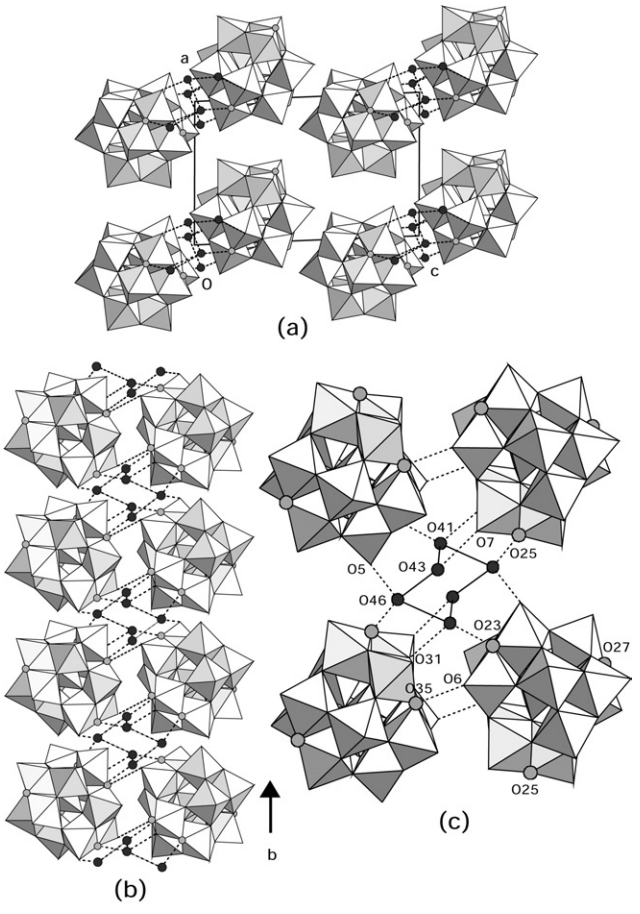

Fig. 5 Compound **1**: (a) crystal packing of polyanions along the [010] direction; (b) chain of polyanions along the *b* axis showing the hydrogen bond network; (c) detailed view of chair conformation of water molecules involved in the polyanion connection. Gray circles denote polyanion protonated oxygens, black circles indicate water molecules.

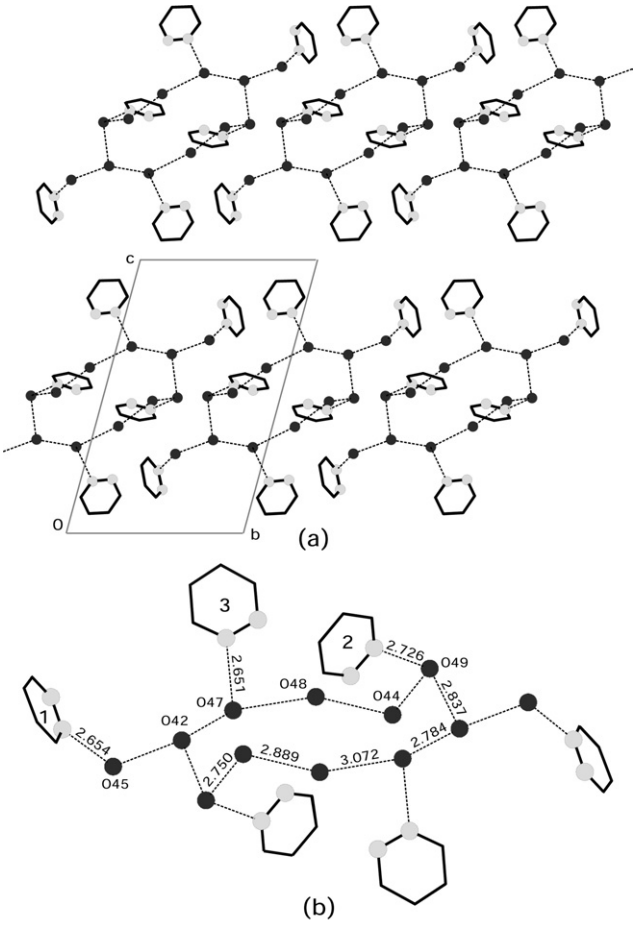

Fig. 6 Compound **1**: (a) crystal packing of cations along the [100] direction; (b) detail of the centrosymmetric ten-membered ring with hydrogen bond distances (Å). Gray circles denote nitrogen atoms, black circles indicate water molecules.

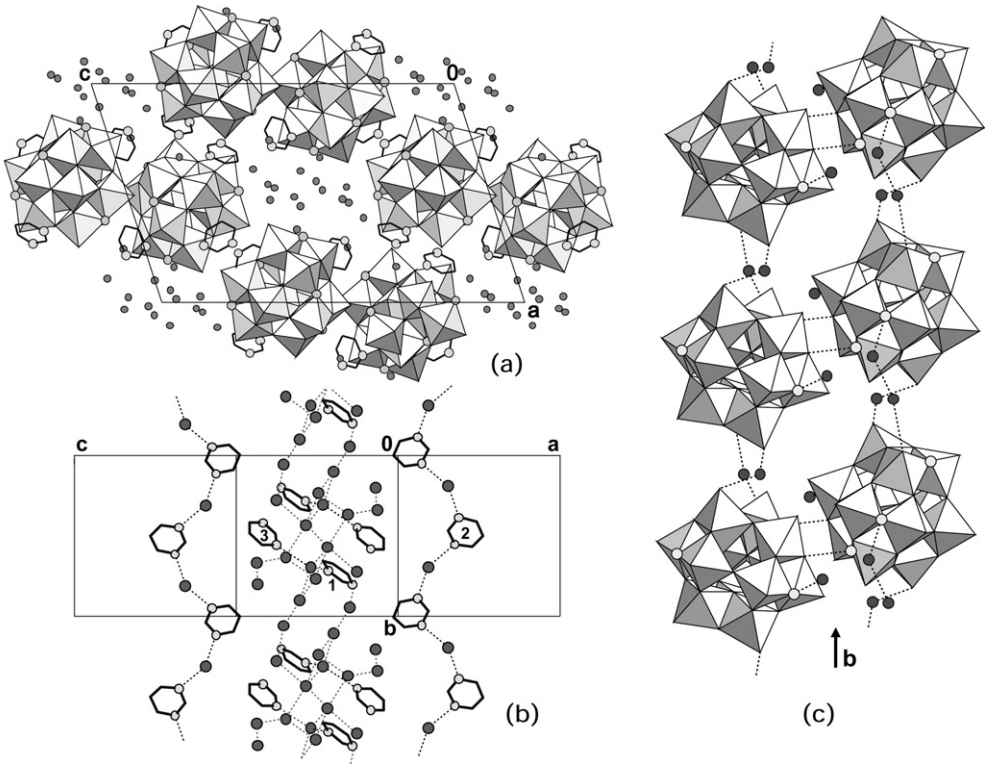

Fig. 7 Compound **2**: (a) crystal packing along the [001] direction; (b) arrangement of 1,3-diazine species around the ''water fall''; (c) view of antiparallel chains of polyanions hydrogen bonded along the [010] direction.

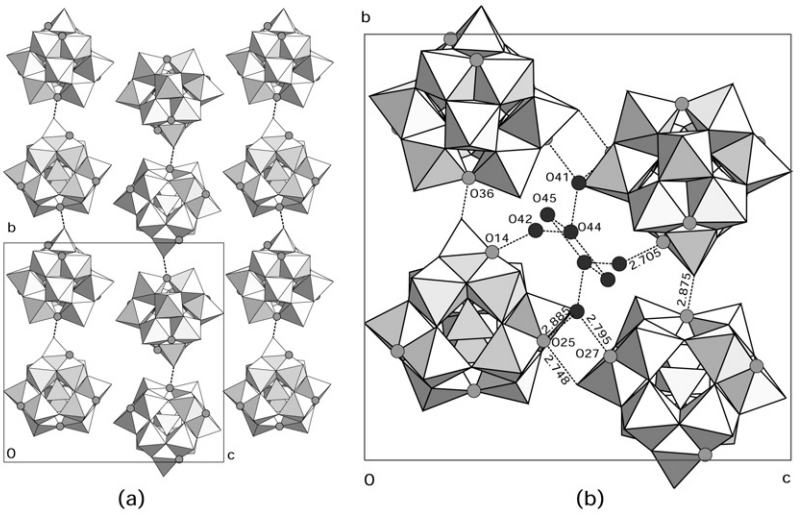

Fig. 8 Compound **6**: (a) view of antiparallel chains of polyanions hydrogen bonded along the [010] direction; (b) unit cell view and water molecules environment with hydrogen bond distances (Å). Gray circles denote polyanion protonated oxygens, black circles indicate water molecules.

3D-tunnel network of hydrogen bonds, because both nitrogen atoms of 1,4-diazine species are involved in the formation of end-on hydrogen bonds. On the other hand in compound **1** only one of the nitrogens is connected to the ten-membered ring of hydrogen bonded water molecules.

The experimental arrangement of organic cations over the tetrameric units of polyanions together with the AIM analysis of the interactions between both moieties suggest that these compounds are good models to explain the interaction between organic substrates and catalyst oxide surfaces.

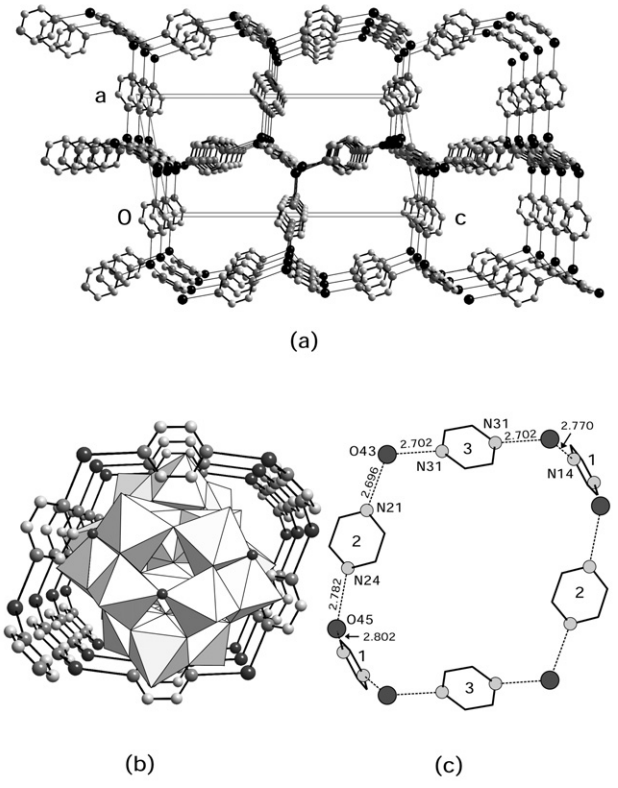

Fig. 9 Compound **6**: (a) perspective view of 1,4-diazine species along the [010] direction showing the tunnel structure where the chains of polyanions are embedded; (b) view of helicoidal arrangement, around a chain of Keggin polyanions, of 1,4-diazine species hydrogen bonded by water molecules. (c) dimensions (Å) and nomenclature in the diazine helicoidal arrangement.

Experimental

Materials

Sodium molybdate dihydrate ($Na_2MO_4{\cdot}2H_2O$, Fluka), sodium hydrogen phosphate (Na_2HPO_4, Aldrich), sodium thiophosphate decahydrate ($Na_3PO_3S{\cdot}10H_2O$, Aldrich), pyridazine (1,2-$C_4H_4N_2$, Aldrich), pyrimidine (1,3-$C_4H_4N_2$, Fluka), pyrazine (1,4-$C_4H_4N_2$, Fluka), 32% hydrochloric acid (HCl, Merck), acetonitrile (CH_3CN, Aldrich), and methanol (CH_3OH, Merck) were used as purchased without further purification. Diazonium chlorhydrates were prepared by passing an HCl gas stream through an organic solution of the corresponding diazine.

Instrumentation

Infrared spectra for solid samples were obtained as KBr pellets, and for photolyte solutions were performed using a drop

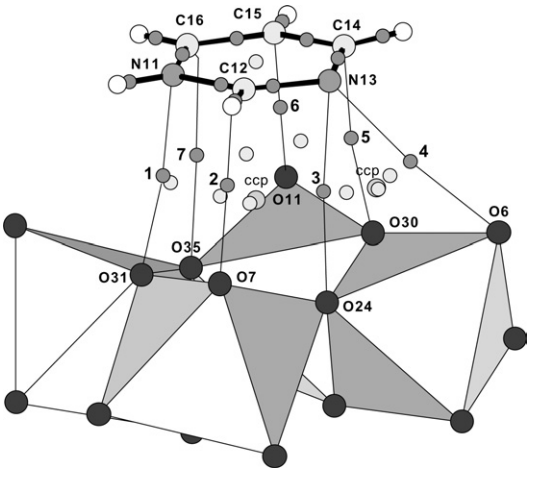

Fig. 10 Molecular graphs determined by the topology of the electron density for the interaction between ring 1 and the corresponding tetramer in compound **2**. Positions of the bond and ring CPs are denoted by dark grey and light grey dots, respectively. The cage CPs are labelled as ccp.

Table 4 Properties of the critical points in the electron density interaction between ring 1 and the corresponding tetramer in compound **2**

Critical point[a]	From···to[b]	Distance/Å	ρ^c	$\nabla^2\rho^d$	ε^e	Type
1	N11···O31	3.01	0.00918	0.03251	0.4772	π–π
2	H12···O7	2.92	0.00335	0.01637	0.5784	H-bond (vw)
3	N13···O24	3.27	0.00580	0.02188	0.5860	π–π
4	N13···O6	3.34	0.00478	0.01859	0.2946	π–π
5	C14···O30	2.94	0.00924	0.03470	0.7498	π–π
6	C15···O11	3.24	0.00587	0.02260	0.5834	π–π
7	C16···O35	3.35	0.00452	0.01841	1.5527	π–π

[a] Labels of critical points as in Fig. 10. [b] Bond path. [c] Electronic density (atomic units). [d] Laplacian. [e] Ellipticity.

of solution between KBr pellets on a Mattson 1000 FT-IR spectrometer. Thermogravimetric studies were performed using 8–15 mg samples in a TA Instruments SDT2960 instrument under a 100 mL min^{-1} flow of synthetic air; the temperature was ramped from 20 to 600 °C at a rate of 5 °C min^{-1} for the decomposition. An Oriel 66032 500 W superhigh-pressure mercury lamp was used as UV-source in the photochemical reactions.

Syntheses

Two general methods were followed in the preparation of the compounds:

Method A, photochemical reduction. An aqueous solution (40 mL) of $Na_2MO_4{\cdot}2H_2O$ (1.0 g, 4.1 mmol) and Na_2HPO_4 (0.057 g 0.40 mmol) was acidified with HCl to pH = 0, then 10 mL of methanol were added. The resulting yellow solution was irradiated in a Schlenk tube (Ø = 20 mm) for 24 h under an atmosphere of nitrogen using a 500 W superhigh-pressure mercury lamp. Addition of the corresponding acidified aqueous solution of diazine (0.165 g, 2.1 mmol) to the dark photolyte produced a fine dark-blue precipitate, which was removed by filtration on a Grade 3 glass sinter. The solids were then washed with water and diethyl ether. Single crystals of compound **1** were obtained by recrystallisation from acetonitrile. Anal. Calcd. for $C_{12}H_{19}Mo_{12}N_6O_{40}P{\cdot}9H_2O$ (**1**): C 6.46; H 1.67; N 3.77%. Found: C 6.37; H 1.65; N 3.71%. Anal. Calcd. for $C_8H_{15}Mo_{12}N_4O_{40}P{\cdot}10H_2O{\cdot}C_4H_4N_2$ (**2**): C 6.41; H 1.75; N 3.74%. Found: C 6.77; H 1.57; N 4.03%. Anal. Calcd. for $C_{12}H_{19}Mo_{12}N_6O_{40}P{\cdot}5H_2O$ (**3**): C 6.67; H 1.43; N 3.89%. Found: C 6.74; H 1.49; N 3.86%.

Method B, chemical reduction. An acidified (pH = 0) aqueous solution (100 mL) of $Na_2MO_4{\cdot}2H_2O$ (3.5 g, 14.5 mmol) and $Na_3PO_3S{\cdot}10H_2O$ (0.48 g 1.21 mmol) was heated with stirring until its colour became dark blue. The sulfur formed was removed by filtration. Addition of the corresponding

Table 5 Crystal data and data collection parameters for compounds **1**, **2** and **6**

	1	**2**	**6**
Formula	$C_{12}H_{19}Mo_{12}N_6O_{40}P{\cdot}9H_2O$	$C_{12}H_{19}Mo_{12}N_6O_{40}P{\cdot}10H_2O$	$C_{10}H_{17}Mo_{12}N_5O_{40}P{\cdot}5H_2O$
Molecular weight	2231.69	2249.71	2119.59
System	Triclinic	Monoclinic	Monoclinic
Space group	$P\bar{1}$	$P2_1/n$	$P2_1/c$
a/Å	12.688(2)	17.149(3)	10.182(1)
b/Å	12.853(11)	12.036(2)	21.356(3)
c/Å	18.597(27)	27.041(5)	21.703(3)
α/°	72.04(9)		
β/°	79.75(12)	107.92	100.55(1)
γ/°	62.95(9)		
V/Å^3	2567(6)	5311(2)	4639(1)
Z	2	4	4
F(000)	2124	4188	4004
D_x/g cm^{-3}	2.887	2.814	3.035
μ/mm^{-1}	2.983	2.885	3.285
Shape	Prism	Prism	Prism
Colour	dark-blue	dark-blue	dark-blue
Size	0.30 × 0.33 × 0.34	0.45 × 0.21 × 0.50	0.25 × 0.31 × 0.34
Diffractometer	Enraf-Nonius CAD4	STOE IPSD	Enraf-Nonius CAD4
Temperature/K	295(1)	293(1)	295(1)
Radiation/Å	0.71069	0.71073	0.71069
Monochromator	Graphite	Graphite	Graphite
Scan mode	ω–2θ	ϕ oscillation	ω–2θ
θ-range/°	2–30	2–25	1–30
hkl	−17 17; −17 18; 0 26	−20 19; −13 13;0 32	−14 14; 0 29; 0 30
Independent reflect.	14 863	9023	13 454
Observed reflections	13 239 [$I \geqslant 2\sigma(I)$]	6392 [$I \geqslant 2\sigma(I)$]	10 780 [$I \geqslant 2\sigma(I)$]
No. variables	721	585	658
Average (Δ/σ)	0.001	0.001	0.005
$R(F^2)$	0.048	0.106	0.049
$wR(F^2)$ (all data)	0.134	0.287	0.139
R(int)	—	0.146	—

diazonium chlorhydrate (0.15 g) yielded a dark-blue precipitate, which was removed by filtration and then was washed with water and diethyl ether. Single crystals of compound **6** were obtained by recrystallisation from a water/ethanol mixture (1:1). Anal. Calcd. for $C_{16}H_{23}Mo_{12}N_8O_{40}P\cdot 2H_2O$ (**4**): C 8.79; H 1.25; N 5.13%. Found: C 8.64; H 1.17; N 4.98%. Anal. Calcd. for $C_{16}H_{23}Mo_{12}N_8O_{40}P\cdot 2H_2O$ (**5**): C 8.79; H 1.25; N 5.13%. Found: C 8.66; H 1.19; N 4.96%. Anal. Calcd. for $C_8H_{15}Mo_{12}N_4O_{40}P\cdot 5H_2O\cdot\frac{1}{2}C_4H_4N_2$ (**6**): C 5.67; H 1.28; N 3.30%. Found: C 5.31; H 1.21; N 3.12%.

Crystallography

Single-crystals suitable for X-ray analysis were obtained for compounds **1**, **2** and **6**. Structural measurements for compounds **1** and **6** were performed on an Enraf-Nonius CAD-4 diffractometer (graphite monochromated MoK_α radiation, $\lambda = 0.71069$ Å). The data were collected at 22 ± 1 °C using the ω–2θ scan technique up to 60° in 2θ. Data collection for the black single crystals of **2** was performed on a STOE IPDS diffractometer, equipped with graphite monochromated MoK_α radiation ($\lambda = 0.71073$ Å). Indexes and unit-cell refinement were based on all observed reflections from ten frames collected with an oscillation range of 1° $frame^{-1}$ and exposure time of 3 min $frame^{-1}$. The intensity data were corrected for Lorentz and polarization effects. Neutral atom scattering factors and anomalous dispersion factors were taken from the literature.[19] Experimental details and crystal data for all three compounds are given in Table 5.

The structures were solved using direct methods.[20] Non-hydrogen atoms were refined anisotropically by full-matrix least-squares analysis and hydrogen atoms of the diazine species were placed in calculated positions. SHELXL97[21] was used for structure refinement of the compounds.

CCDC reference numbers 188194–188196. See http://www.rsc.org/suppdata/nj/b2/b207243b/ for crystallographic data in CIF or other electronic format.

Computational details

All calculations were performed using the Gaussian 98W program.[22] The geometry optimisations of the α- and β-isomers of the Keggin anion in idealised T_d and C_{3v} symmetry, respectively, were performed at the RHF level of theory employing the LANL2DZ basis set, which includes the Huzinaga–Dunning double-ζ basic set[23] for the oxygen atoms, and the Hay and Wadt effective core potentials,[24] accounting for the Mo relativistic effects, with a double-ζ valence basis set for phosphorus and molybdenum atoms. The calculation of the model including a ring cation and a tetrameric unit of the Keggin anion was performed at the RHF level of theory, with the LANL2DZ ECP and basis set on Mo, and 6-31+G* on all the other atoms.

The AIM analysis of the charge density was done with Morphy1.0.[25]

Acknowledgements

This work was supported by Ministerio de Educación y Cultura (Grant No. PB98/0238).

References

1 M. T. Pope and A. Müller, *Angew. Chem., Int. Ed. Engl.*, 1991, **30**, 34; *Polyoxometalates: From Platonic Solids to Antiretroviral Activity*, ed. M. T. Pope and A. Müller, Kluwer, Dordrecht, The Netherlands, 1994*Polyoxometalate Chemistry: From Topology via Self-Assembly to Applications*, ed. M. T. Pope and A. Müller, Kluwer, Dordrecht, The Netherlands, 2001.

2 M. Misono, *Catal. Rev. Sci. Eng.*, 1988, **30**, 339; N. Mizuno and M. Misono, *J. Phys. Chem.*, 1990, **94**, 890; M. Misono and N. Nojiri, *Appl. Catal.*, 1990, **64**, 1; K. Y. Lee, T. Arai, S. Nakata, S. Asaoka, T. Okuhara and M. Misono, *J. Am. Chem. Soc.*, 1992, **114**, 2836; I. V. Kozhevnikov and K. I. Matveev, *Appl. Catal.*, 1983, **5**, 135; R. Newmann and M. Lissel, *J. Org. Chem.*, 1989, **54**, 4607; T. Ilkenhaus, B. Herzorg, T. Braun and R. Schlögl, *J. Catal.*, 1995, **153**, 275; R. Belanger and J. B. Moffat, *J. Catal.*, 1995, **152**, 171; A. Corma, *Chem. Rev.*, 1995, **95**, 559; I. V. Kozhevnikov, *Catal. Rev. Sci. Eng.*, 1995, **37**, 311; I. A. Weinstock, *Chem. Rev.*, 1998, **98**, 113; I. V. Kozhevnikov, *Chem. Rev.*, 1998, **98**, 171; N. Mizuno and M. Misono, *Chem. Rev.*, 1998, **98**, 199; R. Neumann, *Progr. Inorg. Chem.*, 1998, **47**, 317; T. Okuhara, N. Mizuno and M. Misono, *Adv. Catal.*, 1996, **41**, 113; L. I. Kuznetsova, G. M. Maksimov and V. A. Likholobov, *Kinet. Catal.*, 1999, **40**, 622; E. Papaconstantinou, *Trends Photochem. Photobiol.*, 1994, **3**, 139.

3 C. L. Hill, M. S. Weeks and R. F. Schinazi, *J. Med. Chem.*, 1990, **33**, 2767; Y. Inouye, Y. Tale, Y. Tokutake, T. Yoshida, A. Yamamoto, T. Yamase and S. Nakamura, *Chem. Pharm. Bull.*, 1990, **38**, 285; T. Yamase, M. Fujita and K. Fukushima, *Inorg. Chim. Acta*, 1988, **151**, 15; G. Chottard, M. Michelon, M. Hervé and G. Hervé, *Biochim. Biophys. Acta*, 1987, **916**, 402; J. T. Rhule, C. L. Hill, D. A. Judd and R. F. Schinazi, *Chem. Rev.*, 1998, **98**, 327; N. Fukuda, T. Yamase and Y. Tajima, *Biol. Pharm. Bull.*, 1999, **22**, 463.

4 C. J. Gómez-García, E. Coronado and L. Ouahab, *Angew. Chem., Int. Ed. Engl.*, 1992, **31**, 240; E. Coronado and C. J. Gómez-García, *Comments Inorg. Chem.*, 1995, **17**, 255; E. Coronado and C. J. Gómez-García, *Chem. Rev.*, 1998, **98**, 273; J. M. Clemente-Juan and E. Coronado, *Coord. Chem. Rev.*, 1999, **193–195**, 361; L. Ouahab, *Chem. Mater.*, 1997, **9**, 1909; L. Ouahab, *Coord. Chem. Rev.*, 1998, **178–180**, 1501; E. Coronado, J. R. Galán-Mascarós, C. Giménez-Sáiz and C. J. Gómez-García, *Adv. Mater. Opt. Electron.*, 1998, **8**, 61; D. G. Kurth, P. Lehmann, D. Volmer, A. Muller and D. Schwahn, *J. Chem. Soc., Dalton Trans.*, 2000, 3989; M. Clemente-León, E. Coronado, P. Delhaes, C. J. Gómez-García and C. Mingolaud, *Adv. Mater.*, 2001, **13**, 574; T. Yamase, *Chem. Rev.*, 1998, **98**, 307; T. Yamase and H. Naruke, *J. Phys. Chem. B*, 1999, **103**, 8850.

5 D. E. Katsoulis, *Chem. Rev.*, 1998, **98**, 359.

6 J. F. Keggin, *Proc. R. Soc. London, Ser. A*, 1934, **144**, 75; R. Strandberg, *Acta Chem. Scand. A*, 1975, **29**, 359.

7 C. L. Hill and M. Prosser-Mccartha, *Coord. Chem. Rev.*, 1995, **143**, 407.

8 E. Papaconstantinou, *Chem. Soc. Rev.*, 1989, **18**, 1; A. Hiskia, A. Mylonas and E. Papaconstantinou, *Chem. Soc. Rev.*, 2001, **30**, 62.

9 *Selectivity in Catalysis*, ed. M. E. Davis and S. L. Suib, ACS Symposium Series, vol. 517, ACS, Washington DC, 1993.

10 R. Schöllhorn, *Chem. Mater.*, 1996, **8**, 1747; S. L. Suib, *Chem. Rev.*, 1993, **93**, 803; A. Müller, H. Reuter and S. Dillinger, *Angew. Chem., Int. Ed. Eng,.*, 1995, **34**, 2328.

11 M. Ugalde, J. M. Gutiérrez-Zorrilla, P. Vitoria, A. Luque, A. S. J. Wery and P. Román, *Chem. Mater.*, 1997, **9**, 2869.

12 L. A. Gribov and W. J. Orville-Thomas, *Theory and Methods of Calculation of Molecular Spectra*, John Wiley and Sons, Chichester, 1988.

13 Y. P. Jeannin, *Chem. Rev.*, 1998, **98**, 51.

14 S. H. Wang and S. A. Jansen, *Chem. Mater.*, 1994, **6**, 2130; E. Ishikawa and T. Yamase, *Bull. Chem. Soc. Jpn.*, 2000, **73**, 641; C-H. Wu, C-Z. Lu, X. Lin, W-B. Yang, H-H. Zhuang and J-S. Huang, *Acta Crystallogr., Sect. E*, 2001, **57**, m390.

15 J. N. Barrows, G. B. Jameson and M. T. Pope, *J. Am. Chem. Soc.*, 1985, **107**, 1771.

16 J. M. Gutiérrez-Zorrilla, PhD Thesis, Universidad del País Vasco, Bilbao, 1984.

17 X. Lopez, J. M. Maestre, C. Bo and J-M. Poblet, *J. Am. Chem. Soc.*, 2001, **123**, 9571.

18 E. Coronado and C. J. Gómez-García, in *Polyoxometalates: From Platonic Solids to Antiretroviral Activity,* ed. M. T. Pope and A. Müller, Kluwer, Dordrecht, The Netherlands, 1994, p. 129.

19 *International Tables for X-ray Crystallography*, Kynoch Press, Birmingham, England, 1974, vol. IV.

20 P. T. Beurkens, G. Admiraal, G Beurkens, W. P. Bosman, S. Garcia-Granda, R. O. Gould, J. M. M. Smits and C. Smykalla, The DIRDIF program system, Technical Report of the Crystallography Laboratory, University of Nijmegen, The Netherlands, 1992.

21 G. M. Sheldrick, SHELXL97, Program for crystal structure refinement, University of Göttingen, Germany, 1997.
22 M. J. Frisch, G. W. Trucks, H. B. Schlegel, G. E. Scuseria, M. A. Robb, J. R. Cheeseman, V. G. Zakrzewski, J. A. Montgomery, R. E. Stratmann, J. C. Burant, S. Dapprich, J. M. Millam, A. D. Daniels, K. N. Kudin, M. C. Strain, O. Farkas, J. Tomasi, V. Barone, M. Cossi, R. Cammi, B. Mennucci, C. Pomelli, C. Adamo, S. Clifford, J. Ochterski, G. A. Petersson, P. Y. Ayala, Q. Cui, K. Morokuma, D. K. Malick, A. D. Rabuck, K. Raghavachari, J. B. Foresman, J. Cioslowski, J. V. Ortiz, B. B. Stefanov, G. Liu, A. Liashenko, P. Piskorz, I. Komaromi, R. Gomperts, R. L. Martin, D. J. Fox, T. Keith, M. A. Al-Laham, C. Y. Peng, A. Nanayakkara, C. Gonzalez, M. Challacombe, P. M. W. Gill, B. G. Johnson, W. Chen, M. W. Wong, J. L. Andres, M. Head-Gordon, E. S. Replogle and J. A. Pople, Gaussian 98W (Revision A.7), Gaussian, Inc., Pittsburgh PA, 1998.
23 T. H. Dunning and P. J. Hay Jr., in *Modern Theoretical Chemistry*, ed. H. F. Schaefer III, Plenum, New York, 1976.
24 P. J. Hay and W. R. Wadt, *J. Chem. Phys.*, 1985, **82**, 299.
25 P. L. A. Popelier, *Comput. Phys. Commun.*, 1996, **93**, 212.